

Temperature and irradiance impacts on the growth, pigmentation and photosystem II quantum yields of *Haematococcus pluvialis* (Chlorophyceae)

Terence J. Evens · Randall P. Niedz ·
Gary J. Kirkpatrick

Received: 24 July 2007 / Revised and Accepted: 9 October 2007 / Published online: 12 December 2007
© Springer Science + Business Media B.V. 2007

Abstract The microalga *Haematococcus pluvialis* Flotow has been the subject of a number of studies concerned with maximizing astaxanthin production for use in animal feeds and for human consumption. Several of these studies have specifically attempted to ascertain the optimal temperature and irradiance combination for growth of *H. pluvialis*, but there has been a great deal of disagreement between laboratories. “Ideal” levels of temperature and irradiance have been reported to range from 14 to 28°C and 30 to 200 $\mu\text{mol photons m}^{-2} \text{s}^{-1}$. The objective of the present study was to simultaneously explore temperature and irradiance effects for a single strain of *H. pluvialis* (UTEX 2505) across an experimental region that encompassed the reported “optimal” combinations of these factors for multiple strains. To this end, a two-dimensional experimental design based on response surface methodology (RSM) was created. Maximum growth rates for UTEX 2505 were achieved at 27°C and 260 $\mu\text{mol photons m}^{-2} \text{s}^{-1}$, while maximum quantum yield for stable charge separation at PSII (F_v/F_m) was achieved at 27°C and 80 $\mu\text{mol photons m}^{-2} \text{s}^{-1}$. Maximum pigment concentrations correlated closely with maximum F_v/F_m . Numeric optimization of growth rate and F_v/F_m produced an optimal combination of 27°C and 250 $\mu\text{mol photons m}^{-2} \text{s}^{-1}$. Polynomial models

of the various response surfaces were validated with multiple points and were found to be very useful for predicting several *H. pluvialis* UTEX 2505 responses across the entire two-dimensional experimental design space.

Keywords Algal physiology · Design of experiments · DOE · Microalgae · Multivariate

Introduction

The green alga *Haematococcus pluvialis* Flotow (Chlorophyceae) is a unicellular freshwater biflagellate (zoospore) that has received a great deal of attention in the past ca. 25 years, primarily because this alga is capable of synthesizing and accumulating large quantities of the ketocarotenoid astaxanthin (3,3'-dihydroxy- β,β -carotene-4,4'-dione). Astaxanthin is the preferred pigment for use in the feed of salmonid fish (Foss et al. 1984; Schiedt et al. 1985), crustaceans (Meyers and Latscha 1997) and poultry (Inborr 1998), and has been investigated for antioxidant activities (Di Mascio et al. 1991; Miller et al. 1996; Rao et al. 2007) and several other nutraceutical applications (cf. Margalith 1999; Lorenz and Cysewski 2000; Guerin et al. 2003).

Haematococcus pluvialis has a complex life cycle consisting of at least three distinct stages (Elliot 1931; Kobayashi et al. 1997). Under optimal conditions the cells are bi-flagellate, spherical to ellipsoid and are enclosed by a cell wall (Santos and Mesquita 1984). Under irradiance, temperature and/or nutrient stress the flagellated cells cease to be motile and gradually encyst through a green resting cell into aplanospores, which develop a distinctive red color due to the accumulation of astaxanthin in free lipid droplets in the cytoplasm (Boussiba 2000). Reproduction is usually by cell division, although cysts containing many daughter

T. J. Evens (✉) · R. P. Niedz
USDA-ARS, U.S. Horticultural Research Laboratory,
Ft. Pierce, FL 34945, USA
e-mail: terence.evens@ars.usda.gov

T. J. Evens · G. J. Kirkpatrick
Mote Marine Laboratory,
Sarasota, FL 34236, USA

cells may be observed (Kobayashi et al. 1997). It has been reported that significant astaxanthin production is not exclusive to aplanospores but may also be demonstrated in vegetative cells (Lee and Ding 1994; Chaumont and Thèpenier 1995; Grünwald et al. 1997), although maximal carotogenesis appears to occur after cell division has ceased.

Generally, the conditions that favor rapid growth rates do not favor astaxanthin accumulation and *vice versa*. This fact has led many researchers to adopt a two-stage approach to mass cultivation of *H. pluvialis* (Fábregas et al. 2003; Olaizola 2000; Boussiba et al. 1999), while others have strived to achieve a culturing strategy where growth and astaxanthin accumulation are simultaneously maximized (Del Rio et al. 2005). There have been multiple studies addressing the optimal conditions for inducing astaxanthin accumulation (Boussiba et al. 1999; Boussiba and Vonshak 1991; Goodwin and Jamikorn 1954; Harker et al. 1996; Kobayashi et al. 1991, 1993; Lee and Soh 1991; etc.), several that have been focused on achieving high biomass (Borowitzka et al. 1991; Domínguez-Bocanegra et al. 2004; Fábregas et al. 2000; Harker et al. 1995; Torzillo et al. 2005), and a few studies have specifically addressed the optimal conditions for vegetative growth (Cifuentes et al. 2003; Del Rio et al. 2005; Gong and Chen 1997; Fan et al. 1994; Jeon et al. 2006; Moya et al. 1997).

However, there is considerable disagreement concerning the optimal temperature and irradiance for achieving maximum vegetative growth rates and/or biomass of *H. pluvialis*. “Ideal” temperatures and irradiances have been reported to range from 14 to 28°C and 30 to 200 $\mu\text{mol photons m}^{-2} \text{ s}^{-1}$ for a variety of strains/isolates from multiple culture collections. This type of disparity is not uncommon in scientific endeavors, but it leads to a great deal of confusion when attempting to compare results for different strains/isolates between laboratories. The objective of this study is to present an experimental framework for determining the optimal temperature and irradiance combination to 1) maximize *H. pluvialis* growth rates, pigmentation, and PSII quantum yield and; 2) facilitate a valid inter-comparison of various, strain-specific responses.

Materials and methods

Culture conditions *Haematococcus pluvialis* Flotow (UTEX 2505) was obtained from the Culture Collection of Algae at the University of Texas at Austin, USA. Cultures were grown in modified Bold’s Basal Medium (mBBM) made from a combination of autoclaved and filter sterilized stock solutions. The mBBM ionic constituents were: 185 μM BO_3^{3-} , 170 μM Ca^{2+} , 770 μM Cl^- , 1.7 μM Co^{2+} , 6.3 μM Cu^{2+} , 171 μM EDTA^{4-} , 17.9 μM Fe^{2+} , 2.71 mM

K^+ , 304 μM Mg^{2+} , 7.3 μM Mn^{2+} , 4.9 μM Mo^{2+} , 3.37 mM Na^+ , 3.63 mM NO_3^- , 1.38 mM PO_4^{3-} , 344 mM SO_4^{2-} , and 30.7 μM Zn^{2+} (all values are total ionic concentrations within the bulk medium and do not reflect any speciation that may occur in solution). The medium recipe was calculated with ARS-Media software (Niedz and Evens 2006). Cultures were grown as semi-continuous batches in 50 mL of mBBM in 150 mL Erlenmeyer flasks in temperature controlled incubators under an 18:6 light:dark irradiance regime. Incubator temperatures were monitored by an internal digital temperature probe and by a thermometer placed in a 150 mL flask filled with 50 mL of water. Illumination was provided by cool-white fluorescent lights. Scalar PAR irradiance (E_0) levels were determined with a 4π spherical micro quantum sensor (Heinz-Walz US-SQS/B) placed within a stoppered 150 mL flask and immersed in 50 mL of H_2O . Cell counts were carried out microscopically using an Improved Neubauer hemacytometer. Cell numbers were kept at $<6 \times 10^4$ cells mL^{-1} by periodic dilution to minimize self-shading and to assure that nutrient levels remained relatively constant. Cultures were acclimated to experimental conditions for a minimum of 4–6 generational cycles before the commencement of the experiments. During this acclimation phase the cultures were diluted with fresh media as soon as they had at least doubled the initial cell density. Relative growth rates (μ) were calculated in early log phase only, before self-shading could become greater than ca. 10% (determined empirically by measuring the irradiance levels inside the culture flasks — data not shown). Dilutions occurred approximately every 2–3 days with an initial target cell density of 1×10^4 cells mL^{-1} .

Chlorophyll fluorescence Maximum quantum yield for stable charge separation at PSII (F_v/F_m) was measured via the saturation pulse method (Schreiber et al. 1986; Schreiber and Bilger 1993) with a Phyto-PAM (Heinz-Walz PHYTO-C equipped with a PHYTO-ED emitter-detector unit). Cells were removed from the incubators ca. 2–3 h after the start of the photoperiod and dark-acclimated for 15 minutes prior to analysis. Values of F_v/F_m (Genty et al. 1989; Havaux et al. 1991) were calculated according to the following equation:

$$F_v/F_m = (F_m - F_0)/F_m \quad (1)$$

where F_m and F_0 are the maximum and minimum fluorescence, respectively, measured on dark-acclimated cells (Butler 1978). F_v/F_m was measured using a 200 ms flash from the LEDs integral to the Phyto-PAM; adjusting the flash intensity and/or flash duration did not increase the maximum fluorescence level.

HPLC pigments Samples for pigment determination were collected on 25 mm, GF/F glass fiber filters (nominal pore size 0.7 μm) by vacuum filtration and stored at -80°C until extraction. Filters were extracted in approximately 1.5 mL of cold 98:2 methanol:0.5 M ammonium acetate, sonicated in an ice bath and placed in the freezer (-20°C) for approximately two hours. The extract was clarified by refrigerated centrifugation and placed in amber vials in a refrigerated auto-injector (SIL-10A, Shimadzu, Inc). The HPLC protocol was conducted according to Van Heukelem and Thomas (2001) utilizing a solvent flowrate of 1.1 mL min^{-1} through an Eclipse XDB-C8 Column (150 \times 4.6 mm, 3.5 μm) maintained at 60°C . Chromatographic peaks were detected by a photodiode array UV-VIS detector (SPD-M10AVP, Shimadzu, Inc.) and identified by retention time and comparison of absorbance spectra with spectra of pigments from authentic standards. Pigment samples were not de-esterified prior to analysis (Yuan and Chen 1997); therefore, astaxanthin was analyzed semi-quantitatively by adding all of the astaxanthin-ester peaks together.

Experimental design The primary objective was to determine the optimal combination of irradiance and temperature for maximizing the growth rate of the UTEX 2505 strain of *H. pluvialis*. The basic strategy was to 1) create a 2-dimensional experimental design space with irradiance (E_0) and temperature (T) representing the two dimensions; 2) grow UTEX 2505 on a set of treatment combinations represented as points distributed on the surface of the design space; 3) generate prediction equations that describe growth, pigmentation, and F_v/F_m over the experimental design space; and 4) test the prediction equations by growing UTEX 2505 at T- E_0 combinations not included in the original design and comparing the measured responses to the responses predicted by the model.

Specifically, sufficient T- E_0 combinations or ‘design points’, 15 in total, were selected with Design Expert software (v7.0.3, Stat-Ease, Inc. Minneapolis, MN) using D-optimality criteria for providing the most accurate estimates of the model coefficients to satisfy a quartic polynomial model (Box and Draper 1971; Myers and Montgomery 2002). The non-linear quartic model generated by Design Expert is of the form:

$$Y = \beta_0 + \beta_1 X_1 + \beta_2 X_2 + \beta_{12} X_1 X_2 + \beta_{11} X_1^2 + \beta_{22} X_2^2 + \beta_{112} X_1^2 X_2 + \beta_{122} X_1 X_2^2 + \beta_{111} X_1^3 + \beta_{222} X_2^3 + \beta_{1122} X_1^2 X_2^2 + \beta_{1112} X_1^3 X_2 + \beta_{1222} X_1 X_2^3 + \beta_{1111} X_1^4 + \beta_{2222} X_2^4 \quad (2)$$

where Y represents the response associated with each factor level combination, β_0 the intercept, and β_1 – β_{2222} are the regression coefficients of the factors X_1 (i.e., T) and X_2 (i.e., E_0).

In addition to those needed to satisfy the model terms, several points, 11 in total, were added to estimate the lack of fit (LOF) between the response surface model and datum points not used to generate the model (Weisberg 1985). A number of points were duplicated in order to: 1) attain sufficient degrees of freedom (df) to estimate pure error across the design space (14 treatments); 2) provide estimates of block effects (5 treatments); and 3) to reduce the potential effect(s) of high leverage points (2 treatments).

Treatments were blocked on temperature and each block was grown in one of two incubators. A subset of treatments was grown in both incubators and the responses were analyzed by t-test to look for significant differences between the two incubators. Lack of significance was taken to indicate that the observed effects were due to temperature and/or irradiance and not to inter-incubator variation.

Statistical analyses R^2 is reported as a measure of the amount of variation around the mean explained by the model. However, R^2 can become biased if extraneous model terms are introduced. Therefore, the adjusted- R^2 (R_{adj}^2), which decreases as the number of terms in the model increases if those additional terms don’t add value to the model, was calculated as:

$$R_{\text{adj}}^2 = 1 - ((n - 1)/n - p) \cdot (1 - R^2) \quad (3)$$

where n is the sample size and p is the number of model terms. Predicted- R^2 (R_{pred}^2), a measure of the amount of variation in new data explained by the model, was calculated as:

$$R_{\text{pred}}^2 = 1 - (\text{PRESS}/\text{SS}_{\text{Total}}) \quad (4)$$

where PRESS is the “prediction error sum of squares” (Allen 1971). PRESS is calculated by removing a single observation from the model, predicting that response point with the remaining $n-1$ observations, repeating this process for all observations, and then summing the squares of the n PRESS residuals (cf. Myers and Montgomery 2002).

For each response (e.g. growth rate, F_v/F_m , pigmentation) all possible models from the mean to sixth-order polynomial were calculated with Design Expert. Initial model selection was based on: a) a lack of any aliased terms, b) low residuals, c) a low p-value, d) significant lack of fit, e) a low standard deviation, f) high R^2 , R_{adj}^2 and R_{pred}^2 , g) close agreement between R_{adj}^2 and R_{pred}^2 , and h) a low PRESS value in relation to the other models. The selected model was then further evaluated according to a battery of adequacy tests as described by Anderson and Whitcomb (2005). Normality was determined by examining a normal probability plot of the internally studentized residuals and assuring that the residuals fit closely to a straight line. Constant variance was determined by plotting the internally

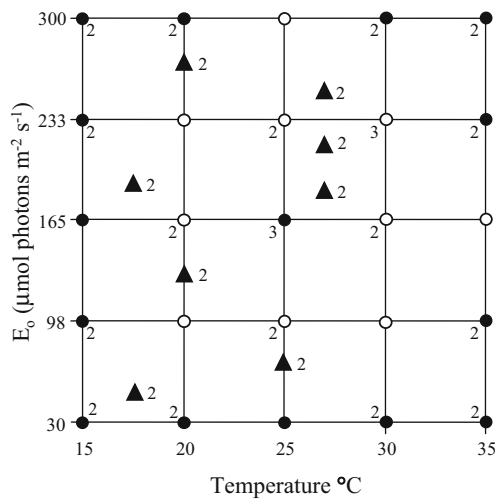


Fig. 1 The two-dimensional design space utilized for this study. T- E_0 combinations used to quantify response surface model coefficients (i.e., ‘model points’) are indicated by the black circles. T- E_0 combinations used to reduce the influence of high leverage points and to quantify block effects and the lack of fit (LOF) of the model(s) derived from the ‘model points’ are indicated by the white circles. T- E_0 combinations used to validate the response surface model’s predictive capabilities are indicated by the black triangles. The number of replicates for each treatment is indicated next to that treatment

studentized residuals versus the predicted responses. If the points fell within an interval of ± 3 standard deviations (σ) and exhibited a constant range of residuals across the graph then constant variance was assumed. A Box-Cox plot for selecting the correct power law transformation was created by generating a curve of the natural log of the sum of squares of the residuals (Box and Cox 1964); a transformation was deemed necessary based on the best lambda value, which is the nadir of the generated curve. “DFFITs” (defined as the change in the predicted value for a point, obtained when that point is left out of the regression) and “DFBETAS” (defined as a normalized measure of the effect of observations on the estimated regression coefficients) plots were used to identify overly influential points (Belsley et al. 1980); points that fell outside $\pm 2\sigma$ were considered suspect (Montgomery et al. 2001; Myers 1990). Adequate precision of the model was determined by comparing the range of the predicted values at the design points (\hat{y}) to the average variance ($V\text{-bar}$) of the prediction (Anderson and Whitcomb 2005). Potential outlier points were checked with externally studentized “outlier-t” (Weisberg 1985; Myers 1990) and Cook’s Distance (Cook and Weisberg 1982) graphical plots.

Model validation In order to empirically assess the usefulness of the predictive capabilities of the proposed RSM models, a variety of validation points were grown in regions of the design space not included in the initial experiments. In addition, a multi-variate optimization technique (Nelder and Mead 1965; Derringer and Suich

1980) was used to identify the region of optimal growth for *H. pluvialis* by simultaneously maximizing μ and F_v/F_m ; three validation points were grown in and near this region (Fig. 1). Two additional validation points were grown in a third incubator (not used in any previous experiments) to further test the assumption about inter-incubator variation. Cultures were grown at all of these points and the measured responses were compared to the predictions. All responses falling within the 95% prediction interval (PI; Hahn and Meeker 1991) were considered as successful validations.

Results

No deviation from normality was detected for any of the measured responses. The variances appeared constant as all points fell within $\pm 3\sigma$ and the scatter did not reveal any

Table 1 ANOVA, model diagnostics and regression coefficient data for growth rate ($\mu \text{ d}^{-1}$) and F_v/F_m

Source	Growth rate	Regression	F_v/F_m	Regression
	p-Values	Coefficients	p-values	Coefficients
Model	<0.0001	0.910	<0.0001	0.720
Temperature (T)	0.0005	0.200	<0.0001	0.058
Irradiance (E_0)	0.0004	0.200	<0.0001	−0.028
T· E_0	0.017	0.230	0.096	0.010
T^2	0.005	−0.470	<0.0001	−0.048
E_0^2	0.756	−0.049	0.027	0.023
$T^2 \cdot E_0$	<0.0001	−0.200	<0.0001	−0.025
$T \cdot E_0^2$	0.516	−0.025	<0.0001	−0.022
T^3	<0.0001	−0.500	<0.0001	−0.120
E_0^3	0.747	0.017	0.005	0.010
$T^2 \cdot E_0^2$	0.005	0.200	0.0001	0.019
$T^3 \cdot E_0$	0.004	−0.220	<0.0001	−0.024
$T \cdot E_0^3$	0.636	−0.034	0.023	0.011
T^4	0.288	−0.150	<0.0001	−0.088
E_0^4	0.370	−0.130	0.003	−0.029
Lack of Fit	0.004		0.068	
Model	Quartic		Quartic	
Transformation	n/a		n/a	
CV %	12.34		0.71	
PRESS	0.30		0.002	
R^2	0.97		1.00	
R_{adj}^2	0.95		1.00	
R_{pred}^2	0.94		0.99	
Precision	23.76		97.56	
Mean	0.59		0.67	
Std. Dev.	0.073		0.005	

Statistically significant p-values (<0.05) are in boldface. Regression coefficients are in terms of coded factors; those listed as “Model” are the intercept terms

obvious distortions. The predicted versus measured plots indicated very close correlations between the modeled and measured data points. The outlier-t and Cook's distance plots did not reveal any data points that could be considered as outliers and therefore suspect. The DFFITS and DFBETAS plots did not indicate any treatments with overly large influences on predictions or regression coefficients, respectively. There were no significant block effects or inter-incubator effects (data not shown).

A summary of the ANOVA data, model diagnostics and coded regression coefficients is presented in Tables 1 and 2. Attempts at model reduction by backward elimination (Nelder 1998; Peixoto 1990) resulted in extremely minor improvements in the model diagnostics for μ , F_v/F_m , Chl *a* and Chl *b*. Therefore, no model reductions were used for these responses and all model terms were included in the ANOVA analyses. The model for total carotenoid concentration was improved by model reduction and is hereafter referred to as a “reduced cubic” model. For clarity, only statistically significant ($p < 0.05$) coefficients are included in

the polynomial equations detailed below. The models for all of the responses were highly significant ($p < 0.0001$), indicating significant factor effects, and were considered of sufficient quality to navigate the experimental design space.

The maximal region for UTEX 2505 growth rate (μ) centers at the T- E_0 combination of [27°C, 260 $\mu\text{mol photons m}^{-2} \text{ s}^{-1}$] and F_v/F_m is maximal near the combination [27°C, 80 $\mu\text{mol photons m}^{-2} \text{ s}^{-1}$] (Fig. 2). Maximal Chl *a* concentrations (Fig. 3) for this strain are produced at [27°C, 35 $\mu\text{mol photons m}^{-2} \text{ s}^{-1}$], while total carotenoids at [29°C, 30 $\mu\text{mol photons m}^{-2} \text{ s}^{-1}$] and maximal Chl *b* can be found at [28°C, 33 $\mu\text{mol photons m}^{-2} \text{ s}^{-1}$] (data not shown for Chl *b*; all concentrations are pg pigment cell⁻¹). Unlike μ and F_v/F_m it is not clear whether the chosen parameter ranges have captured the actual maximum pigment concentration responses for UTEX 2505, because the pigment levels are maximal near the minimum irradiance ‘edge’ of the design space. The present experimental design would need to be augmented to extend E_0 to lesser values in order to determine if maximal pigment levels have been reached.

Table 2 ANOVA, model diagnostics and regression coefficient data for Chl *a*, Chl *b* and total carotenoid concentrations (pg pigment cell⁻¹)

Source	Chl <i>a</i>	Regression	Chl <i>b</i>	Regression	Carot.	Regression
	p-Values	Coefficients	p-Values	Coefficients	p-Values	Coefficients
Model	<0.0001	0.100	<0.0001	0.570	<0.0001	0.710
Temperature (T)	<0.0001	-0.084	<0.0001	-0.410	0.0001	-0.550
Irradiance (E_0)	0.001	0.064	<0.0001	0.340	<0.0001	0.230
T· E_0	0.540	-0.020	<0.0001	-0.190	0.005	-0.170
T ²	0.711	0.020	<0.0001	0.330	0.002	0.24
E_0^2	0.503	0.037	0.246	-0.043		
T ² · E_0	0.462	0.010	0.348	-0.050		
T · E_0^2	0.869	0.002	0.622	0.026		
T ³	<0.0001	0.15	<0.0001	0.480	<0.0001	0.680
E_0^3	0.609	0.009	0.181	-0.099		
T ² · E_0^2	0.431	0.019				
T ³ · E_0	0.019	-0.061				
T · E_0^3	0.115	0.040				
T ⁴	0.146	0.074				
E_0^4	0.453	-0.038				
Lack of Fit	0.023		0.029		0.149	
Model Transformation	Quartic Power ^{-1.52}		Cubic Inverse		Red. Cubic Power ^{-1.84}	
CV %	16.92		14.48		24.74	
PRESS	0.039		0.57		2.09	
R ²	0.93		0.89		0.65	
R _{adj} ²	0.90		0.86		0.60	
R _{pred} ²	0.87		0.83		0.54	
Precision	16.84		17.95		11.73	
Mean	0.15		0.71		0.82	
Std. Dev.	0.025		0.10		0.20	

Statistically significant p-values (<0.05) are in boldface. Regression coefficients are in terms of coded factors; those listed as “Model” are the intercept terms

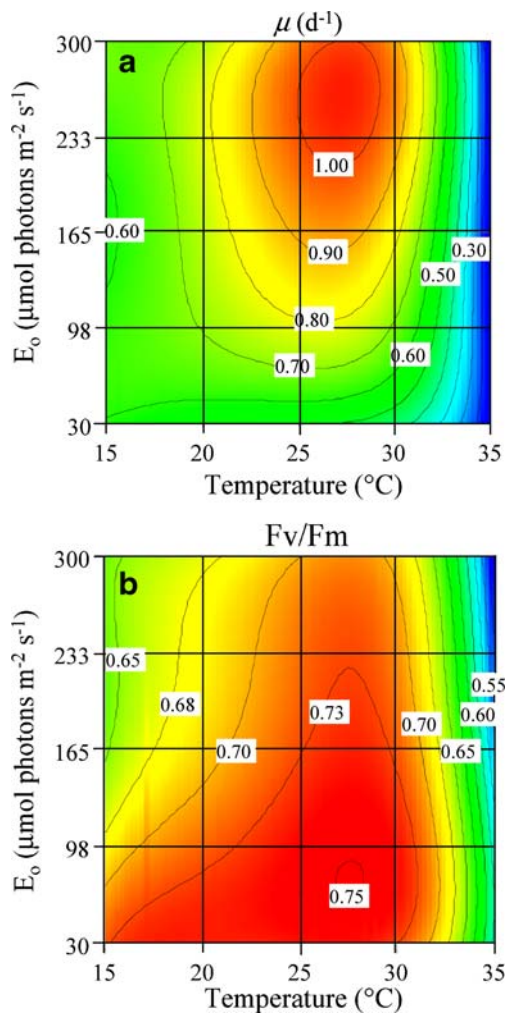


Fig. 2 Two-dimensional contour of μ (a) and F_v/F_m (b) response surfaces. The color scales are indicated by the contour lines and are unique to each plot

Relative growth rates The 35°C treatments did not grow, even after methodical and rigorous attempts to acclimate the cultures to this temperature. Therefore, in order to maintain the mathematical integrity of the RSM models, μ for these treatments were recorded as “zero” for “no growth”. The R^2_{adj} and R^2_{pred} values are quite high for μ , and show close agreement, which indicates that the chosen model performs well in prediction and is reasonably robust to point deletion (Fig. 2). The precision for the chosen model indicates that the signal-to-noise ratio of the data is adequate for these analyses. The coefficient of variation (CV) for this response is low, indicating close agreement between duplicated measurements. The ANOVA revealed nine significant quartic model terms, which includes both of the linear terms, all of the quadratic terms (except for E_0^2), two cubic ($T^2 \cdot E_0$ and T^3) and two quartic ($T^2 \cdot E_0^2$ and $T^3 \cdot E_0$) terms. The LOF term for μ was also significant (Table 1).

The quartic polynomial in terms of actual factors that describes μ across the T- E_0 design space is as follows:

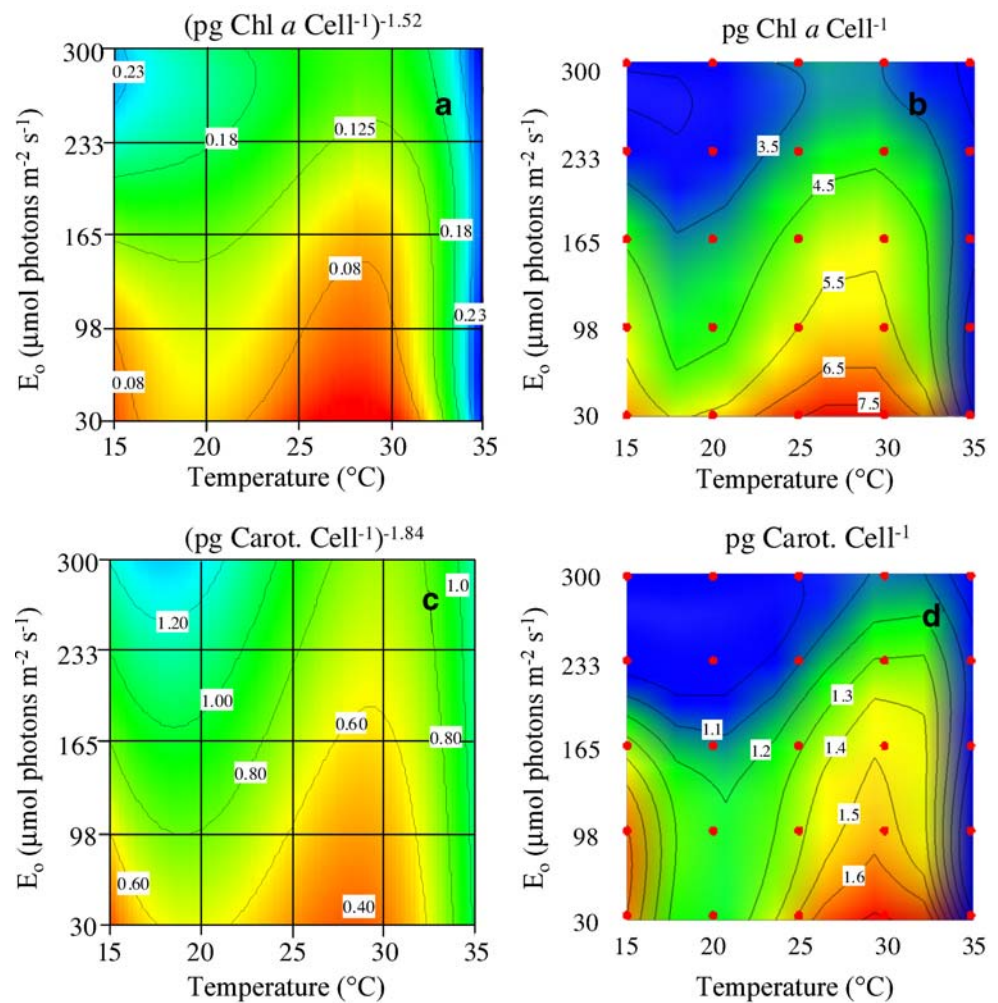
$$\begin{aligned} \mu = & -1.51 + 0.48 \cdot T + 4.60E-4 \cdot E_0 \\ & - 3.57E-4 \cdot (T \cdot E_0) - 0.04 \cdot T^2 \\ & + 6.99E-5 \cdot (T^2 \cdot E_0) + 1.31E-3 \cdot T^3 \\ & + 1.11E-7 \cdot (T^2 \cdot E_0^2) - 1.62E-6 \cdot (T^3 \cdot E_0) \end{aligned} \quad (5)$$

F_v/F_m The R^2_{adj} and R^2_{pred} values are extremely high for F_v/F_m , and show close agreement (Fig. 2). The precision for the chosen model indicates that the signal-to-noise ratio of the data is adequate for these analyses. The CV for this response is low, indicating very close agreement between duplicated measurements. The LOF term for F_v/F_m is not significant. The only non-significant model term for F_v/F_m is the quadratic interaction term, T- E_0 (Table 1). The quartic polynomial in terms of actual factors that describes F_v/F_m is:

$$\begin{aligned} F_v/F_m = & -1.26 + 0.38 \cdot T - 1.31E-3 \cdot E_0 - 0.03 \cdot T^2 \\ & + 2.31E-8 \cdot E_0^2 + 8.23E-6 \cdot (T^2 \cdot E_0) \\ & - 8.69E-7 \cdot (T \cdot E_0^2) \cdot T^3 + 7.89E-4 \cdot T^3 \\ & + 5.10E-8 \cdot E_0^3 + 1.06E-8 \cdot (T^2 \cdot E_0^2) \\ & - 1.81E-7 \cdot (T^3 \cdot E_0) + 4.47 \cdot (TE_0^3) \\ & - 8.76E-6 \cdot T^4 - 8.79E-11 \cdot E_0^4 \end{aligned} \quad (6)$$

Pigmentation Pigments identified from *H. pluvialis* include Chl *a*, Chl *b*, 9-cis-neoxanthin, violaxanthin, antheraxanthin, zeaxanthin, β - β carotene, and astaxanthin. Trace amounts of Chl *a* allomers and epimers were detected on occasion. Astaxanthin concentrations varied across the design space, but were never found in amounts that would be of interest for commercial uses. Therefore, pigments were separated into three groups for response surface modeling, Chl *a*, total carotenoids (defined as the sum of all the carotenoids except astaxanthin; Fig. 3) and Chl *b*. Pigment values for the 35°C treatments were very low and extremely noisy and, as such were considered unreliable. Pigment concentrations (reported as pg pigment cell⁻¹) were therefore averaged across all treatments for this temperature in order to maintain the mathematical integrity of the RSM models. The R^2_{adj} and R^2_{pred} values for Chl *a* and Chl *b* concentrations show close agreement and leave only ca. 10% of the variance unexplained by the models. The precision for the chosen models indicates that the signal-to-noise ratios of the data are adequate for these analyses. The CVs for these responses are higher than μ and F_v/F_m , indicating lesser agreement between replicate samples. The Box-Cox plots indicated that Chl *a* and Chl *b* required a power and an inverse transformation, respectively. The

Fig. 3 Two-dimensional, transformed response surfaces and fitted raw data contour plots of Chl *a* (**a**, **b**) and total carotenoid (Carot.; **c**, **d**) concentrations. The color scales are indicated by the labeled contour lines and are unique to each plot



LOF terms for Chl *a* and Chl *b* are significant (Table 2). The quartic polynomial in terms of actual factors that describes the Chl *a* concentration response surface is:

$$[\text{Chl } a]^{-1.52} = 0.07 - 0.08 \cdot T + 3.21E - 3 \cdot E_0 - 5.12E - 4 \cdot T^3 - 4.54E - 7 \cdot (T^3 \cdot E_0). \quad (7)$$

The cubic polynomial in terms of actual factors that describes the Chl *b* response surface is:

$$[\text{Chl } b]^{-1} = -4.42 + 0.69 \cdot T + 2.51E - 3 \cdot E_0 - 5.81E - 6 \cdot (T \cdot E_0) - 0.03 \cdot T^2 + 4.76E - 4 \cdot T^3. \quad (8)$$

The backward elimination of non-significant total carotenoid model terms used an “alpha to exit” value of 0.10; model hierarchy was maintained at all times (Myers and Montgomery 2002). The R_{adj}^2 and R_{pred}^2 values for total carotenoid concentrations show close agreement but are

lower than the other responses reported in this study, indicating that the model fits the data poorly and should be used for prediction with some caution. The precision for the chosen model indicates that the signal-to-noise ratio of the data is adequate. The CV for this response is fairly high in relation to the other responses, indicating a greater variance for replicate samples. The LOF term for total carotenoid concentration is not significant (Table 2). The reduced cubic polynomial in terms of actual factors that describes the total carotenoid concentration response surface is:

$$[\text{Carot.}]^{-1.84} = -7.93 + 1.13 \cdot T + 4.88E - 3 \cdot E_0 - 1.26E - 4 \cdot (T \cdot E_0) - 0.05 \cdot T^2 + 6.84E - 4 \cdot T^3. \quad (9)$$

Model validation Predicted μ and F_v/F_m values for the temperature-irradiance (T- E_0) combinations chosen for model validation all fell within the 95% PI with the exception of a single F_v/F_m value (data not shown;

Fig. 4 The total carotenoid/Chl *a* (Carot./Chl *a*) and Chl *b*/Chl *a* ratios for four of the temperatures used in this study. Treatments without error bars are the result of single measurements

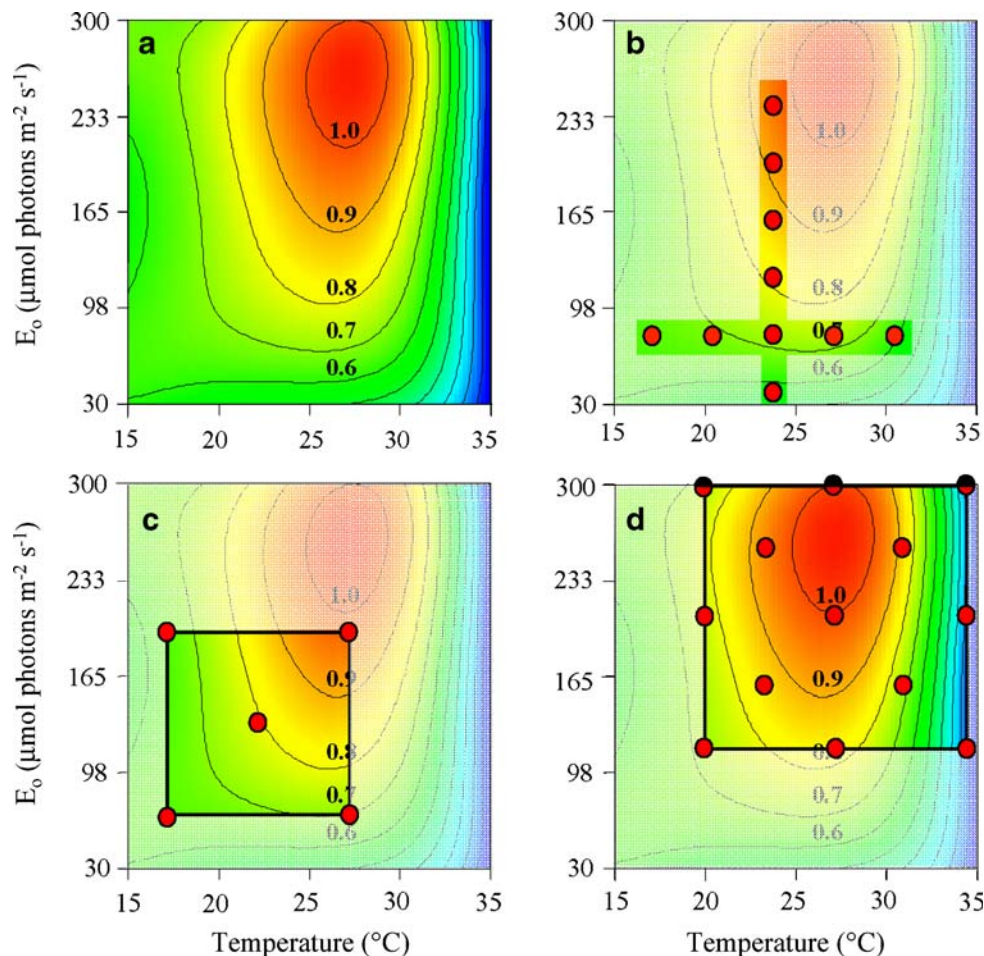
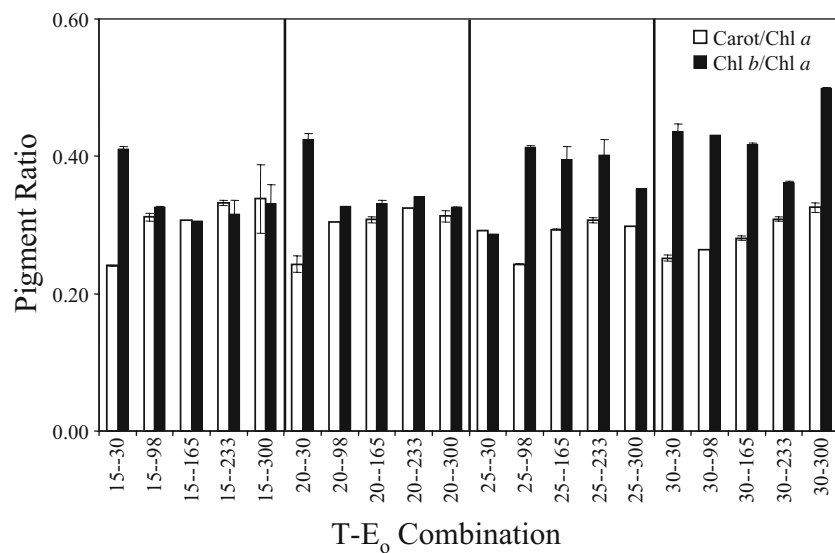


Fig. 5 (a) If it can be assumed that the growth rate response surface quantified for LB2505, then (b) it is obvious that an OFAT approach samples a limited region of this design space. (c) However, if a multivariate approach to quantifying T-E effects/interactions is attempted, but the chosen ranges for the independent factors fail to

include the regions of interest (e.g. maximal μ) then even this approach can prove misleading. (d) It is only by using a multivariate approach and carefully choosing parameter ranges to fully encompass the regions of interest that we can be assured of satisfactorily quantifying the effects and interactions between primary, driving factors such as T and E_0 .

validation treatments indicated on Fig. 1). This indicates that the chosen models describe these response surfaces well and are highly reliable for prediction. Chl *a* and Chl *b* concentrations were predicted reasonably well with six of the eight T- E_o combinations falling within the 95% PI. Surprisingly, despite the weak model diagnostics, total carotenoid concentrations were predicted quite well with seven of the eight predictions falling within the 95% PI; however, due to the poor response surface model fit the prediction intervals were quite large for this response.

A numeric optimization of μ and F_v/F_m was used to simultaneously maximize both of these responses in order to identify the *optimal* region centered at [27°C, 250 $\mu\text{mol photons m}^{-2} \text{s}^{-1}$]. Cultures grown at this T- E_o combination fell within the 95% PIs for all measured responses (data not shown). The fact that the maximal regions for μ and F_v/F_m are at different irradiances along the same temperature axis is of interest. It is also interesting to note how well Chl *a* correlates with F_v/F_m . The contour plots for these two responses are quite similar and their maximal points lie close together. Chl *a* might serve as a reasonable proxy for F_v/F_m and vice versa for UTEX 2505.

Discussion

A wide range of differences in μ , F_v/F_m and pigmentation were observed. The ANOVA results (Tables 1 & 2) and the contour plots (Figs. 2 and 3) indicate that both T and E_o are highly important to the dynamics of these responses, and that there are significant interactions between these two factors. An analysis of the F-values (data not shown) and p-values (Tables 1 & 2) for these responses indicates that temperature is more influential than irradiance across the ranges explored in this study. This is primarily due to the fact that the parameter ranges chosen for this study bracket the extremes of LB2505 acclimation potential better in one dimension (T) than the other (E_o). There are also several highly significant irradiance terms, but most of this factor's influence is seen in the ($T^x \cdot E_o^x$) interaction terms.

The increase in pigment concentrations with decreasing irradiance is consistent with our expectations of this response (c.f. MacIntyre et al. 2002 and Richardson et al. 1983). However, the contour plots of pigmentation responses do not adequately describe all of the dynamic interplay between UTEX 2505 photosynthetic pigments. The total carotenoid/Chl *a* and Chl *b*/Chl *a* ratios exhibit an interesting trend that illustrates the non-linear interactions between T and E_o . Between 15 and 20°C only the 30 $\mu\text{mol photons m}^{-2} \text{s}^{-1}$ cultures exhibit an enhancement of Chl *b* relative to the carotenoid complement (Fig. 4). However, between 25 and 30°C the Chl *b*/Chl *a* ratios are consistently

higher than the total carotenoid/Chl *a* ratios. It is also worth noting the minimal variation in the total carotenoid/Chl *a* ratios across the range of temperatures and irradiances displayed in Fig. 4.

The lack of fit (LOF) terms for μ , Chl *a* and Chl *b* were highly significant. This means that the variation of the replicates about their mean values is less than the variation of the treatment responses about their predicted values. This can indicate that the chosen models do not fit well and/or that replicated points have small variances. Given that: a)

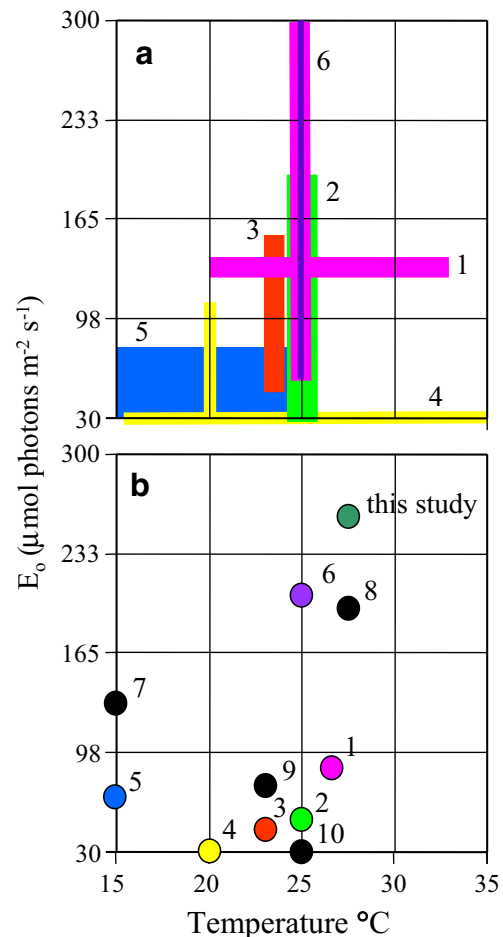


Fig. 6 A synopsis of several studies on various strains/isolates of *H. pluvialis/lacustris* and their relation to the present effort. **(a)** Several studies have explored various sub-regions of the temperature-irradiance parameter space explored in the present study. Six studies* have been selected to illustrate the coverage attained with OFATs and/or constrained RSMs ([1; pink] Fan et al. 1994¹, [2; green] Fábregas et al. 2000, [3; red] Cifuentes et al. 2003, [4; yellow] Hagen et al. 2001², [5; blue] Harker et al. 1995³ and [6; purple] Torzillo et al. 2005⁴). It is apparent that large areas of T-E parameter space have been left unexplored by these studies. **(b)** The temperature-irradiance combination identified as "optimal" and/or chosen for growth of several strains/isolates *H. pluvialis/lacustris* for 10 studies attempting to attain maximal biomass and/or define optimal growth conditions (references as above in (a) plus (7), Gong and Chen 1997, (8) Borowitzka et al. 1991, (9) Domínguez-Bocanegra et al. 2004, and (10) Moya et al. 1997). *Complete ranges for E_{PAR} were ¹50–400, ²0–100, ³10–70 and ⁴50–600 $\mu\text{mol photons m}^{-2} \text{s}^{-1}$

this was the only diagnostic that failed, b) the higher order, aliased polynomials did not exhibit a better LOF, c) a visual examination of the fitted response surface in relation to the measured design points revealed a reasonable agreement between the two, and d) the validation points were predicted with a high degree of accuracy, it was concluded that the LOF was a reliable metric, but did not invalidate the model. A more succinct explanation per George Box (1979) might be that although these models are “wrong” they appear useful for predicting UTEX 2505 physiological responses to T and E_o .

The majority of studies that have attempted to ascertain optimal factor combinations for *H. pluvialis* (and other algae) growth have used a classic one-factor-at-a-time (OFAT) approach that involves setting one factor (e.g., “T”) at some constant value and then varying another factor (e.g., “E”) across a range of interest. A response (e.g., μ) is measured and plotted and the “maximal” point is then used to fix E while varying T; an optimal combination of T-E is then reported. However, this approach presupposes a lack of interaction between the independent factors and relies upon the factor effects exhibiting a linear response in each dimension (cf. Anderson and Whitcomb 2005). If there are interactions between the factors then this approach can lead to spurious conclusions. For instance, if we assume that the growth rate response surface quantified with the present study represents the “true” response surface for UTEX 2505 (Fig. 5a), then it is immediately obvious that an OFAT approach samples a limited region of this design space (Fig. 5b). The results for this type of approach can be highly dependent on the chosen starting levels; if there are interactions between the factors under study then the OFAT approach can lead to the false identification of maximal responses. However, if a multivariate approach to quantifying T-E effects/interactions is attempted, but the chosen ranges for the independent factors fail to include the regions of interest (e.g., maximal μ) then even this approach can prove misleading (Fig. 5c). It is only by carefully choosing parameter ranges to fully encompass the regions of interest and using a multivariate approach that we can be assured of satisfactorily quantifying the effects and interactions between primary, driving factors such as T and E_o (Fig. 5d). The “crossed gradient” approach described by Křiváková and Lukavský (2001) is an elegant approach to achieving multiple temperature/irradiance combinations and should prove very amenable to the application of multivariate experimental designs.

The experimental ranges and reported optimal T-E combinations of ten studies focused on determining the level of T and/or E for maximum growth rates and/or biomass accumulation are illustrated in Fig. 6. This highlights the difficulty of exploring a relatively large, feasible experimental design space with the OFAT approach or with

a poorly constrained RSM. Optimal T-E combinations reported to be used for vegetative growth/biomass accumulation range from 14 to 28°C and 30 to 200 $\mu\text{mol photons m}^{-2} \text{s}^{-1}$. Obviously, a great deal of this variation can be due to species/strain/isolate-specific responses. However, it is also quite possible that the range of optimal responses is heavily influenced by the limitations imposed by the OFAT approach. Until the optimal T-E combinations for these strains are examined in the same context as the present study, we will not know the source of this dramatic range of responses.

Additional confounding aspects of many previous studies include the use of planar (2π) rather than scalar (4π) irradiance sensors and the use of batch rather than semi-continuous or continuous cultures. A 2π sensor can miss significant variations in irradiance levels if careful control of scattered/reflected light within an incubator is not exercised. Batch cultures are convenient, but they present many difficulties, such as nutrient depletion and self-shading, to ascertaining responses to the factors of interest (cf. MacIntyre and Cullen 2005). All of these uncertainties combine to make inter-comparisons between studies of *H. pluvialis* difficult. However, these difficulties can be overcome through careful experimental design and a methodical approach to achieving quantifiable and repeatable culturing conditions.

Acknowledgements We would like to thank Mr. Peter D’Aiuto for excellent technical assistance with culturing *H. pluvialis* and Ms. Rita Bowker for assistance with the HPLC measurements. We would also like to thank the folks at Stat-Ease for the extremely informative discussions on the various statistical aspects of this research. Mention of trade names or commercial products in this article is solely for the purpose of providing specific information and does not imply recommendation or endorsement by the U.S. Department of Agriculture.

References

- Allen DM (1971) Mean square error of prediction as a criterion for selecting variables. *Technometrics* 13:469–475
- Anderson MJ, Whitcomb PJ (2005) RSM simplified: optimizing processes using response surface methods for design of experiments. Productivity Press, New York
- Belsley DA, Kuh E, Welsch RE (1980) Regression diagnostics: identifying influential data and sources of collinearity. Wiley, New York
- Borowitzka MA, Huisman JM, Osborn A (1991) Culture of the astaxanthin-producing green alga *Haematococcus pluvialis*. I. Effects of nutrients on growth and cell type. *J Appl Phycol* 3:295–304
- Boussiba S (2000) Carotenogenesis in the green alga *Haematococcus pluvialis*: cellular physiology and stress response. *Physiol Plant* 108:111–117
- Boussiba S, Vonshak A (1991) Astaxanthin accumulation in the green alga *Haematococcus pluvialis*. *Plant Cell Physiol* 32:1077–1082
- Boussiba S, Bing W, Yuan J-P, Zarka A, Chen F (1999) Changes in pigments profile in the green alga *Haematococcus pluvialis* exposed to environmental stresses. *Biotechnol Lett* 21:601–604

- Box GEP (1979) Robustness in the strategy of scientific model building. In: Launer RL, Wilkinson GN (eds) Robustness in statistics. Academic, New York, pp 201–236
- Box GEP, Cox DR (1964) An analysis of transformations (with discussion). J Royal Statistical Soc Ser B 26:211–246
- Box GEP, Draper NR (1971) Factorial designs, the X^*X criterion, and some related matters. Technometrics 13:731–741
- Butler WL (1978) Energy distribution of the photochemical apparatus of photosynthesis. Annu Rev Plant Physiol 29:345–378
- Chaumont D, Thèpenier C (1995) Carotenoid content in growing cells of *Haematococcus pluvialis* during a sunlight cycle. J Appl Phycol 7:529–537
- Cifuentes AS, González MA, Vargas S, Hoeneisen M, González N (2003) Optimization of biomass, total carotenoids and astaxanthin production in *Haematococcus pluvialis* flotox strain septoe (Nevada, USA) under laboratory conditions. Biol Res 36:343–357
- Cook RD, Weisberg S (1982) Residuals and influence in regression. Chapman Hall, New York
- Del Rio E, Acien G, García-Malea MC, Rivas J, Molina-Grima E, Guerrero MG (2005) Efficient one-step production of astaxanthin by the microalga *Haematococcus pluvialis* in continuous culture. Biotechnol Bioeng 91:808–815
- Derringer G, Suich R (1980) Simultaneous optimization of several response variables. J Qual Technol 12:214–219
- Di Mascio P, Murphy ME, Sies H (1991) Antioxidant defense systems: the role of carotenoids, tocopherols, and thiols. Am J Clin Nutr 53:194S–200S
- Domínguez-Bocanegra AR, Legarreta IG, Jeronimo FM, Campocoso AT (2004) Influence of environmental and nutritional factors in the production of astaxanthin from *Haematococcus pluvialis*. Bioresource Technol 92:209–214
- Elliot AM (1931) Morphology and life history of *Haematococcus pluvialis*. Arch Protistenk 82:250–272
- Fábregas J, Domínguez A, Regueiro M, Maseda A, Otero A (2000) Optimization of culture medium for the continuous cultivation of the microalga *Haematococcus pluvialis*. Appl Microbiol Biotechnol 53:530–535
- Fábregas J, Domínguez A, Maseda A, Otero A (2003) Interactions between irradiance and nutrient availability during astaxanthin accumulation and degradation in *Haematococcus pluvialis*. Appl Microbiol Biotechnol 61:545–551
- Fan L, Vonshak A, Boussiba S (1994) Effect of temperature and irradiance on growth of *Haematococcus pluvialis* (Chlorophyceae). J Phycol 30:829–833
- Foss P, Storebakken T, Schiedt K, Liaaen-Jensen S, Austreng E, Streiff K (1984) Carotenoids in diets for salmonids. I. Pigmentation of rainbow trout with the individual optical isomers of astaxanthin in comparison with canthaxanthin. Aquaculture 41:213–226
- Genty B, Briantais J-M, Baker NR (1989) The relationship between the quantum yield of photosynthetic electron transport and quenching of chlorophyll fluorescence. Biochim Biophys Acta 990:87–92
- Gong X, Chen F (1997) Optimization of culture medium for growth of *Haematococcus pluvialis*. J Appl Phycol 9:437–444
- Goodwin TW, Jamikorn M (1954) Studies in carotogenesis: 11. Carotenoid synthesis in the alga *Haematococcus pluvialis*. Biochem J 57:376–381
- Grünewald K, Hagen C, Braune W (1997) Secondary carotenoid accumulation in flagellates of the green alga *Haematococcus lacustris*. Eur J Phycol 32:387–392
- Guerin M, Huntley ME, Olaiola M (2003) *Haematococcus* astaxanthin: applications for human health and nutrition. Trends Biotechnol 21:210–216
- Hagen C, Grünewald K, Xyländer M, Rothe E (2001) Effect of cultivation parameters on growth and pigment biosynthesis in flagellated cells of *Haematococcus pluvialis*. J Appl Phycol 13:79–87
- Hahn GJ, Meeker WQ (1991) Statistical intervals: a guide for practitioners. Wiley & Sons, New York
- Harker M, Tsavalos AJ, Young AJ (1995) Use of response surface methodology to optimize carotenogenesis in the microalga, *Haematococcus pluvialis*. J Appl Phycol 7:399–406
- Harker M, Tsavalos AJ, Young AJ (1996) Factors responsible for astaxanthin formation in the chlorophyte *Haematococcus pluvialis*. Bioresource Technol 55:207–214
- Havaux M, Strasser RJ, Greppin H (1991) A theoretical and experimental analysis of the q_P and q_N coefficients of chlorophyll fluorescence quenching and their relation to photochemical and nonphotochemical events. Photosynth Res 27:41–55
- Inbarr J (1998) *Haematococcus*, the poultry pigmentor. Feed Mix 6:31–34
- Jeon Y-C, Cho C-W, Yun Y-S (2006) Combined effects of light intensity and acetate concentration on the growth of unicellular microalga *Haematococcus pluvialis*. Enzyme Microbial Technol 39:490–495
- Kobayashi M, Kakizono T, Nagai S (1991) Astaxanthin production by a green alga, *Haematococcus pluvialis* accompanied with morphological changes in acetate media. J Ferment Bioeng 71: 335–339
- Kobayashi M, Kakizono T, Nagai S (1993) Enhanced carotenoid biosynthesis by oxidative stress in acetate-induced cyst cells of a green unicellular alga, *Haematococcus pluvialis*. Appl Environ Microbiol 59:867–873
- Kobayashi M, Kurimura Y, Kakizono T, Nishio N, Tsuji Y (1997) Morphological changes in the life cycle of the green alga *Haematococcus pluvialis*. J Ferment Bioeng 84:94–97
- Kvíderová J, Lukavský J (2001) A new unit of crossed gradients of temperature and light. In: Elster J, Seckbach J, Vincent WF, Lhotsky O (eds) Algae and extreme environments. Nova Hedwigia 123:539–548
- Lee YK, Ding SY (1994) Cell cycle and accumulation of astaxanthin in *Haematococcus lacustris* (Chlorophyta). J Phycol 30: 445–449
- Lee YK, Soh CW (1991) Accumulation of astaxanthin in *Haematococcus lacustris* (Chlorophyta). J Phycol 27:575–577
- Lorenz RT, Cysewski GR (2000) Commercial potential for *Haematococcus* microalgae as a natural source of astaxanthin. Trends Biotechnol 18:160–167
- MacIntyre HL, Cullen JJ (2005) Using cultures to investigate the physiological ecology of microalgae. In: Andersen RA (ed) Algal culturing techniques. Elsevier, London, pp 287–326
- MacIntyre HL, Kana TM, Anning T, Geider RJ (2002) Photoacclimation of photosynthesis irradiance response curves and photosynthetic pigments in microalgae and cyanobacteria. J Phycol 38:17–38
- Margalith PZ (1999) Production of ketocarotenoids by microalgae. Appl Microbiol Biotechnol 51:431–438
- Meyers SF, Latscha L (1997) Carotenoids. In: D'Abramo LR, Conklin DE, Akiyama DM (eds) Crustacean nutrition advances in world aquaculture, vol. 6. The World Aquaculture Society, Baton Rouge, LA, USA, pp 164–186
- Miller NJ, Sampson J, Candeias LP, Bramley PM, Rice-Evans CA (1996) Antioxidant activities of carotenes and xanthophylls. FEBS Lett 384:240–242
- Montgomery DC, Peck EA, Vining GG (2001) Introduction to linear regression analysis, 3rd edn. Wiley, New York
- Moya MJ, Sánchez-Guardamino ML, Vilavella A, Barberà E (1997) Growth of *Haematococcus lacustris*: a contribution to kinetic modeling. J Chem Tech Biotechnol 68:303–309
- Myers RH (1990) Classical and modern regression with applications, 2nd edn. PWS-KENT, Boston

- Myers RH, Montgomery DC (2002) Response surface methodology: process and product optimization using designed experiments, 2nd edn. Wiley, New York
- Nelder JA (1998) The selection of terms in response surface models — how strong is the weak heredity principle? *Am Stat* 52: 315–318
- Nelder JA, Mead R (1965) A simplex method for function minimization. *Comput J* 7:308–313
- Niedz RP, Evens TJ (2006) A solution to the problem of ion confounding in experimental biology. *Nature Methods* 3:417
- Olaizola M (2000) Commercial production of astaxanthin from *Haematococcus pluvialis* using 25,000-liter outdoor photobioreactors. *J Appl Phycol* 12:499–506
- Peixoto J (1990) A property of well-formulated polynomial regression models. *Am Stat* 44:26–30
- Rao AR, Sarada R, Ravishankar GA (2007) Stabilization of astaxanthin in edible oils and its use as antioxidant. *J Sci Food Agric* 87:957–965
- Richardson K, Beardall J, Raven JA (1983) Adaptation of unicellular algae to irradiance: an analysis of strategies. *New Phytol* 93: 157–191
- Santos MF, Mesquita JF (1984) Ultrastructural study of *Haematococcus lacustris* (Girod) Rostafinski (Volvocales). I. Some aspects of carotenogenesis. *Cytologia* 49:215–228
- Schreiber U, Bilger W (1993) Progress in chlorophyll fluorescence research: major developments during the past years in retrospect. *Prog Bot* 54:151–173
- Schiedt K, Leuenberger FJ, Vecchi M, Glinz E (1985) Absorption, retention and metabolic transformations of carotenoids in rainbow trout, salmon and chicken. *Pure Appl Chem* 57: 685–692
- Schreiber U, Schliwa U, Bilber B (1986) Continuous recording of photochemical and non-photochemical chlorophyll fluorescence quenching with a new type of modulation fluorometer. *Photosynth Res* 10:51–62
- Torzillo G, Göksan T, Isik O, Gökpınar S (2005) Photon irradiance required to support optimal growth and interrelations between irradiance and pigment composition in the green alga *Haematococcus pluvialis*. *Eur J Phycol* 40:233–240
- Van Heukelem L, Thomas CS (2001) Computer-assisted high performance liquid chromatography method development with applications to the isolation and analysis of phytoplankton pigments. *J Chrom A* 910:31–49
- Weisberg S (1985) Applied linear regression, 2nd edn. Wiley & Sons, New York
- Yuan J-P, Chen F (1997) Identification of astaxanthin isomers in *Haematococcus lacustris* by HPLC-photodiode array detection. *Biotechnol Techniques* 11:455–459